Brain and Cognition 83 (2013) 72–79

Contents lists available at ScienceDirect

Brain and Cognition

journal homepage: www.elsevier.com/locate/b&c

Case History Study

Developmental dissociation of visual dorsal stream parvo and magnocellular representations and the functional impact of negative retinotopic BOLD responses

Isabel Catarina Duarte [a,b], Gil Cunha [a,b,c], João Castelhano [b], Francisco Sales [c], Aldina Reis [b], João Paulo Silva Cunha [d,a], Miguel Castelo-Branco [a,b,*]

[a] Brain Imaging Network, ICNAS, Azinhaga de Santa Comba, 3000-058 Coimbra, Portugal
[b] Institute for Biomedical Imaging and Life Sciences, IBILI, Azinhaga de Santa Comba, 3000-548 Coimbra, Portugal
[c] Coimbra University Hospital, Praceta Prof. Mota Pinto, 3000-075 Coimbra, Portugal
[d] INESC TEC / Dep. of Electrical and Computer Engineering, Faculty of Engineering, University of Porto, 4200-465 Porto, Portugal

ARTICLE INFO

Article history:
Accepted 10 July 2013

Keywords:
fMRI retinotopic mapping
Visual function
EEG/fMRI
Dorsal stream
Magnocellular pathway
Negative BOLD

ABSTRACT

Localized neurodevelopmental defects provide an opportunity to study structure–function correlations in the human nervous system. This unique multimodal case report of epileptogenic dysplasia in the visual cortex allowed exploring visual function across distinct pathways in retinotopic regions and the dorsal stream, in relation to fMRI retinotopic mapping and spike triggered BOLD responses.

Pre-surgical EEG/video monitoring, MRI/DTI, EEG/fMRI, PET and SPECT were performed to characterize structure/function correlations in this patient with a very early lesion onset. In addition, we included psychophysical methods (assessing parvo/konio and magnocellular pathways) and retinotopic mapping.

We could identify dorsal stream impairment (with extended contrast sensitivity deficits within the input magno system contrasting with more confined parvocellular deficits) with disrupted active visual field input representations in regions neighboring the lesion. Simultaneous EEG/fMRI identified perilesional and retinotopic bilaterally symmetric BOLD deactivation triggered by interictal spikes, which matched the contralateral spread of magnocellular dysfunction revealed in the psychophysical tests. Topographic changes in retinotopic organization further suggested long term functional effects of abnormal electrical discharges during brain development.

We conclude that fMRI based visual field cortical mapping shows evidence for retinotopic dissociation between magno and parvocellular function well beyond striate cortex, identifiable in high level dorsal visual representations around visual area V3A which is consistent with the effects of epileptic spike triggered negative BOLD.

1. Introduction

It is now generally accepted that visual information travels across two main cortical pathways, the dorsal and ventral streams. The former is involved in "vision for action" processing and receives dominant input from the magnocellular system (Thiele, Dobkins, & Albright, 2001; Goodale & Milner, 1992). The ventral stream is involved in "vision for recognition" and receives mixed input from the parvocellular and magnocellular systems (Ungerleider & Haxby, 1994; Goodale & Milner, 1992). Both parallel systems originate in the ganglion cell layer of the retina, but have distinct projections to the lateral geniculate nucleus. The parvocellular system is endowed with better spatial resolution and is color selective; it mainly projects to ventral "what" system, which however receives also substantial magnocellular input. The magnocellular pathway has high temporal resolution, high sensitivity to contrast and is motion sensitive. It is the dominant projection to the "where" dorsal pathway system (Goodale & Milner, 1992; Livingstone & Hubel, 1988).

Invasive and non-invasive studies in non-human primates have allowed the investigation of structure–function correlations in the visual cortex, as well as in the parvo and magno recipient regions in the ventral and dorsal streams. In macaque, visual motion processing is mainly associated with the visual area MT (Newsome & Paré, 1988) and related regions in the dorsal stream, such as V3 and V6 (Galletti et al., 2001; Orban, Van Essen, & Vanduffel,

* Corresponding author. Address: IBILI, Azinhaga de Santa Comba, Celas, 3000-548 Coimbra, Portugal. Fax: +351 239480217.
E-mail addresses: catarinaduarte86@gmail.com (I.C. Duarte), gnv.cunha@gmail.com (G. Cunha), jmscastelhano@gmail.com (J. Castelhano), franciscosales@huc.min-saude.pt (F. Sales), aldinareis@gmail.com (A. Reis), jcunha@ieee.org (J.P.S. Cunha), mcbranco@fmed.uc.pt (M. Castelo-Branco).

0278-2626/$ - see front matter © 2013 Elsevier Inc. All rights reserved.
http://dx.doi.org/10.1016/j.bandc.2013.07.001

2004; Vanduffel et al., 2001). In humans this homology seems to hold, with the notable exception of V3, which is less motion selective than V3A (Tootell et al., 1997).

In humans, functional lesion and neuroimaging studies do provide a unique opportunity to explore these structure–function correlations across streams (Blanke, Landis, Mermoud, Spinelli, & Safran, 2003; Braddick, O'Brien, Wattam-Bell, Atkinson, & Turner, 2000; Castelo-Branco et al., 2006; Vaina et al., 2003). Human V3A has a continuous map of the contralateral hemifield, including a unique representation of the upper visual field (Tootell et al., 1997; Wandell, Dumoulin, & Brewer, 2007; Wandell & Winawer, 2011) and as stated above, is more motion selective in humans than the adjacent V3 area (Braddick et al., 2000; Tootell et al., 1997; Vaina et al., 2003; Wattam-Bell et al., 2010). Both have high sensitivity to contrast (Tootell et al., 1997), which is a typical feature of the magnocellular system.

In the present study, we report a case of developmental dysplasia associated with early onset visual cortical epilepsy. Pre-surgical EEG/video monitoring, MRI/DTI, EEG/fMRI, PET and SPECT were performed to characterize structure/function correlations in this patient. MRI data revealed a cortical dysplasia in the retinotopic cortex, close to the V3d/V3A areas. Due to the lesion location, the patient underwent psychophysical testing to assess chromatic pathways and high temporal/low spatial frequency channels (biased for magnocellular activation) as well as fMRI based field mapping (retinotopy) to better explore the neural underpinnings of the observed functional deficits.

Accordingly, the particular location of this small lesion provided the opportunity to investigate the visual functional dissociation across distinct pathways in retinotopic regions using multimodal methods.

2. Methods

We report a case of a patient with intractable epilepsy in whom multimodal evaluation was performed to clarify and support the medical decision concerning surgery. The study was approved by our local Ethics Committee and was performed after obtaining the patient's written informed consent.

2.1. Patient

The patient was a 21 years old left-handed female. She had no history of familial epilepsy, meningitis, febrile seizures or head trauma. She presented well preserved episodic memory, and a discrete defect in visual episodic memory and visuospatial perception. These defects have small impact on her daily life and do not disable her work as a waitress. Her additional neuropsychological evaluation revealed psychomotor lentification. Neurological examination was otherwise normal. The patient's seizures started at the first month of life, with right asymmetric spasms. Currently, she is having daily seizures only during sleep.

The patient underwent long-term video/EEG monitoring. The scalp interictal EEG showed clusters of repetitive spikes on both parietal-occipital and midline areas. The ictal EEG was non-lateralizing, showing an abrupt cessation of spikes and a build-up of a fast activity, propagating to the left parietal and frontal regions. The ictal semiology started with blinking and moaning as she was feeling fear (suggestive of occipito limbic propagation). This was followed, some seconds after, by a hypermotor pattern (pedal movements) and a tonic asymmetric posture, also suggesting left supplementary sensorimotor area activation.

Interictal PET revealed decreased metabolism in superior left occipital cortex. Ictal and interictal SPECT were concordant with PET, supporting an epileptogenic area located in the superior left occipital cortex.

2.2. MRI measurements

2.2.1. Structural MRI

Patient was scanned using a 3T scanner (Magnetom Trio Tim, Siemens, Germany) and a 12 channel head coil. A T1-weighted MPRAGE sequence was measured with repetition time (TR) 2300 ms, echo time (TE) 2.98 ms, resolution 1 mm^3, flip angle 9°, matrix size 256×256, field of view (FOV) 256×256 and slice thickness 1 mm.

Cortical thickness analysis (CTA) was performed using the structural MPRAGE images and the processing was done in BrainVoyager QX 2.0 (BrainVoyager QX, Brain Innovation, The Netherlands). The analysis, based on the Laplace's equation (Jones, Buchbinder, & Aharon, 2000), starts with the segmentation of the inner and outer cortex boundary to produce the cortex thickness volume maps, which are used to calculate the cortical thickness on surface meshes.

2.2.2. DTI tractography

For DTI (Diehl et al., 2010), a T1-weighted EPI sequence was acquired with 20 diffusion directions, resolution $3 \times 1.8 \times 1.8$ mm^3, TR 5200 ms, TE 104 ms, flip angle 90°, matrix size 128×128, FOV 230×230, and b value of 1000 s/mm^2. The optic radiation tractography was performed using the software FMRIB's Diffusion Toolbox 2.0 (University of Oxford, England).

2.2.3. Retinotopy

A T1-weighted EPI sequence was measured with TR 2000 ms, TE 39 ms, flip angle 90°, resolution 2 mm^3, matrix size 128×128, slice thickness and space between slices of 2.5 mm.

The stimuli consists of a rotating (clockwise and anticlockwise) checkered wedge (flickering at 8 Hz, 8 rotations, period 64s, eccentricity 23°), while the subject fixed a central point (Sereno et al., 1995). The statistical polar angle maps and in particular meridian representations obtained with this stimulus are used to provide the information to delineate the visual areas V1, V2 and V3 in normal subjects.

The stimulus was viewed through a mirror that reflects the image of a LCD projector (Avotec, USA). Functional data analysis was performed also using BrainVoyager QX 2.0. Pre-processing included 3D motion correction, slice scan time correction (cubic spline interpolation) and temporal filtering. The images were aligned to the anatomical volume from where the cortical surface was extracted and inflated. Linear correlation maps were used to map the visual field angular position. This method requires stringent correlation between visual stimulus position and BOLD activity. We expect that no phase locking is present between spiking activity and stimulus onset, leading to averaging out of noisy effects caused by spiking. Moreover, EEG/fMRI mapping of spiking activity was performed in a fully independent session. The cross-correlation was calculated as a function of the time lag (in TR units, 2 s per lag). Lag values at each voxel were encoded in pseudo-colors. Voxels were included into the statistical map if $r > 0.20$ and $p < 0.05$.

2.3. Visual field psychophysical mapping

The patient underwent standard and visual pathway-isolating perimetric psychophysical mapping (Castelo-Branco et al., 2006; Silva et al., 2008). Conventional static white-on-white perimetry (MonCv3, Metrovision, France) was performed to evaluate the function of the central visual field (stimulus Goldmann size III in a background luminance of 10 cd/m^2, testing 76 points regularly spaced every 6 up to 20° eccentricity).

To assess chromatic pathways, blue-on-yellow static perimetry was performed (MonCv3, Metrovision, France), using a blue (440 nm) stimulus, Goldmann size V, generated over an yellow (530 nm) background with a high luminance of 100 cd/m^2.

We performed motion perimetry in the same testing device using the motion-30 stimulus. In this test, the background is dark gray (10 cd/m^2) with 94 white bars with a luminance of 100 cd/m^2, size of 3 × 34 pixels (10 × 100 arc min) with optimized and uniform locations up to 30° eccentricity. The visual field was assessed using as a stimulus the relative local displacement of each bar, and using a rapid thresholding strategy. The displacement changes 0.85 arc min/dB (for a sensitivity of 0 dB the displacement is 30 arc min; for a sensitivity of 30 dB the displacement is 4.5 arc min). The bar performs this horizontal movement during 300 ms and then it returns to its initial position.

All perimetric measures were monitored using an infrared camera which permits the response rejection in case of movement or eye blink.

Patient also underwent a magnocellular-biased contrast-sensitivity test (high temporal/low spatial frequency channel) using the frequency doubling technology (Humphrey-Matrix, Carl Zeiss, Germany). The stimuli are perceptually "frequency doubled" due to the high temporal flicker rate of sinusoidal gratings (18 Hz) at low spatial frequency (0.50 cycle/°), in a mean background luminance of 100 cd/m^2 and a contrast range from 56 to 0 dB. During the perimetry, 19 locations in the central 30° visual field were tested while the subject was instructed to report the detection of "flickering striped" targets. The visual field was divided in four stimulus test locations in each quadrant and includes two additional nasal locations, 10° eccentricity each, and a central circular target which subtended a radius of 5° (Castelo-Branco et al., 2006).

2.4. EEG/fMRI

The EEG/fMRI experiment involved the acquisition of EEG continuous data during 10 min, with a 64 channels MRI-compatible cap (Maglink, Compumedics, USA) and a 10 kHz sampling rate. A whole-brain EPI sequence was acquired, with a resolution of 3 mm^3 and TR of 3000 ms. Pre-processing included 3D motion correction, slice scan time correction (cubic spline interpolation) and temporal filtering (GLM approach with Fourier basis set, 2 cycles/run). Functional data was co-registered with the structural images and analyzed in BrainVoyager QX 2.0 (BrainVoyager QX, Brain Innovation, The Netherlands). EEG signal was pre-processed in EEGLAB (Delorme & Makeig, 2004), a toolbox for MATlab (MathWorks, USA), including gradient and ballistocardiogram artifact removal. The analysis was performed using Scan4.5/Maglink (NeuroScan, Compumedics, USA). The spikes of interictal activity were identified by an epileptologist and the timings were used to create the GLM (General Linear Model) to correlate BOLD signal (convolved with a canonical hemodynamic response function) with the epileptic activity, as in rapid event-related fMRI designs (Marques et al., 2009).

3. Results

Fig. 1A and B illustrates the MR based structural analysis, and shows a cortical dysplasia spanning the left cuneus and precuneus. The dysplastic lesion is centered on the Talairach coordinates $x = -20$, $y = -74$, $z = 15$, and it extends from the slice $x = -28$ to $x = -12$, from $y = -84$ to $y = -64$ and from $z = 0$ to $z = 30$. This location likely affected retinotopic regions around magno recipient visual areas V3A (Tootell et al., 1997; Pitzalis et al., 2006) and V6 (Dechent & Frahm, 2003; Simon & et al., 2002; de Jong, van der Graaf, & Paans, 2001), and likely V3d where both magno and parvo inputs are more balanced.

The tractography revealed a very close spatial relationship between the dysplasia and the left optical radiation (Fig. 1C and D), suggesting a high risk of damage to this radiation in case of surgery.

Figs. 2 and 3 depict the psychophysical impact of retinotopic damage. Despite no clinically detectable deficits, achromatic static white-on-white (Fig. 2, upper) and chromatic blue-on-yellow (Fig. 2, bottom) perimetries, revealed a peripherally confined scotoma dominating in the right inferior quadrant visual field that matches the lesion location in the left superior visual cortex (note black ellipses marking the blind spot (physiological scotoma) regions in each eye, confirming the accuracy of eye position monitoring ensured by the use of an infrared camera which permits response rejection in case of movement or eye blink).

Perimetric testing of the high temporal/low spatial frequency channel (magnocellular-tuned input to the visual dorsal stream function) using both flickering and motion stimuli revealed a surprising pattern in which deficits spanned the whole right hemifield (Fig. 3), consistent of damage of retinotopic areas which are known to represent whole hemifields, beyond quadrants and are magnocellular biased (V3A and V6). Moreover, such extended visual field defects revealed in the magnocellular/motion isolating perimetries showed a surprising and intriguing contralateral expansion of the deficit beyond the right hemifield, including part of the left hemifield (Fig. 3). This suggested contralateral spread of damage, possibly related to contralateral spread of spiking activity (see below).

In the EEG, acquired simultaneously with fMRI, 89 spikes were identified in a 5 min period in the continuous EEG signal by an experienced epileptologist. Analysis of the BOLD signal changes triggered by interictal activity showed a region of negative BOLD in the cortex surrounding the lesion (Fig. 4). Interestingly, the deactivation spreads symmetrically to similar and retinotopically matched visual representations in the contralateral hemisphere, (Fig. 4) corresponding to regions with psychophysically identified visual loss, and corroborating the above documented contralateral spread of functional damage.

Retinotopic mapping revealed a relatively disorganized map in the left visual cortex (see Fig. 5A and B), where only V1 and V2 boundaries and parts of V3 could be identified around the lesion site, since their boundaries were topologically disrupted by asynchronous spiking activity. In the left hemisphere we can note an increase in the V1 extension, as compared to the right hemisphere. This technique also revealed the expected decreased activity in the dysplastic cortex. These results can justify the patient's impairments in visual performance as a consequence of the disrupted retinotopic representations.

Cortical thickness analysis clearly highlights the dysplastic lesion in the left hemisphere (Fig. 5D). The lesion location is consistent with the information from retinotopic data which revealed an absence of activity within this region (Fig. 5C).

4. Discussion

In the present work, we were able to study a patient harboring an early onset neurodevelopmental lesion with a dissociative pattern in visual function and found evidence for high level (dorsal stream) segregation of magnocellular and parvocellular function.

4.1. Relevance of lesion location to understand magnocellular processing in the dorsal stream and the cortical dichotomy of magno versus parvocellular processing

The lesion location was found to be related to the magno recipient visual areas V3d/V3A and possibly V6 (Dechent & Frahm, 2003; Pitzalis et al., 2006). Both these regions have representations

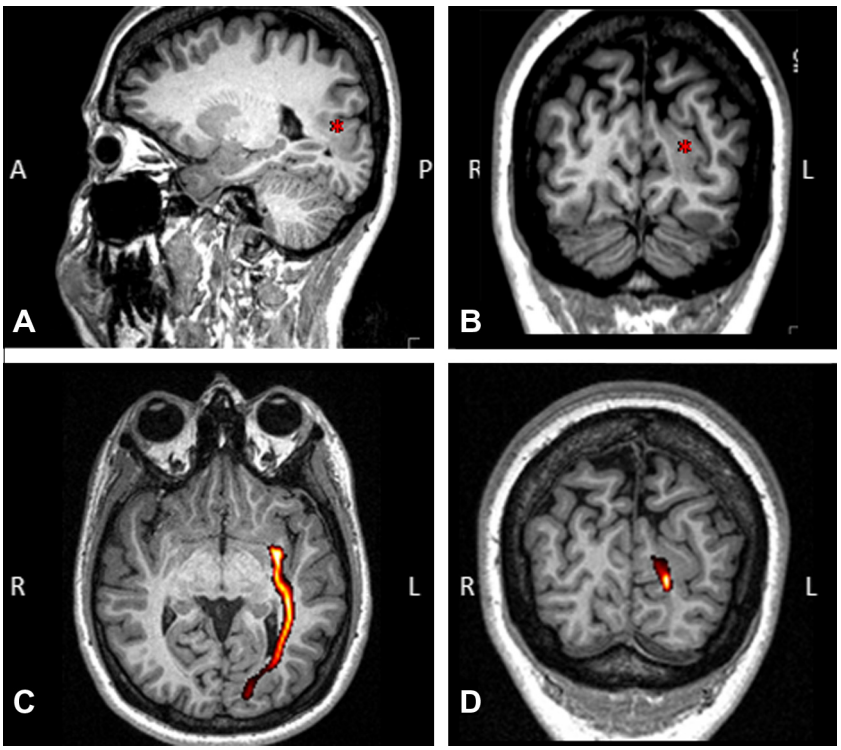

Fig. 1. Structural imaging. (A and B) T1- weighted MPRAGE. MRI revealed a cortical dysplasia, an abnormal thickening of the grey-white matter boundary, in the left cuneus and precuneus occipital region (*). (C and D) Left optical radiation tractography (transversal and coronal).

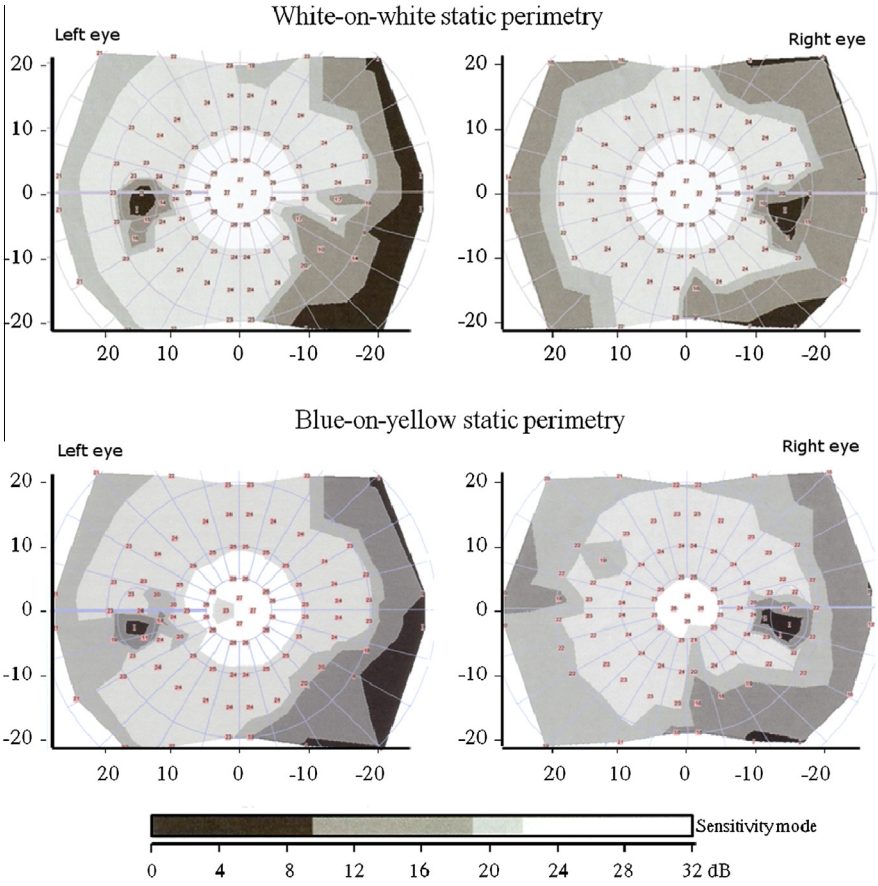

Fig. 2. Visual field static perimetries. Upper: White-on-white static perimetry (non tuned to particular pathways) revealed a peripheral defect mainly in the right inferior visual field. Bottom: Blue-on-yellow (parvo/koniocellular pathway) also showed a defect in the right inferior quadrant. Note that black elliptic regions correspond to blind spot of each eye and should not preclude the interpretation of homonymous impairment. (For interpretation of the references to color in this figure legend, the reader is referred to the web version of this article.)

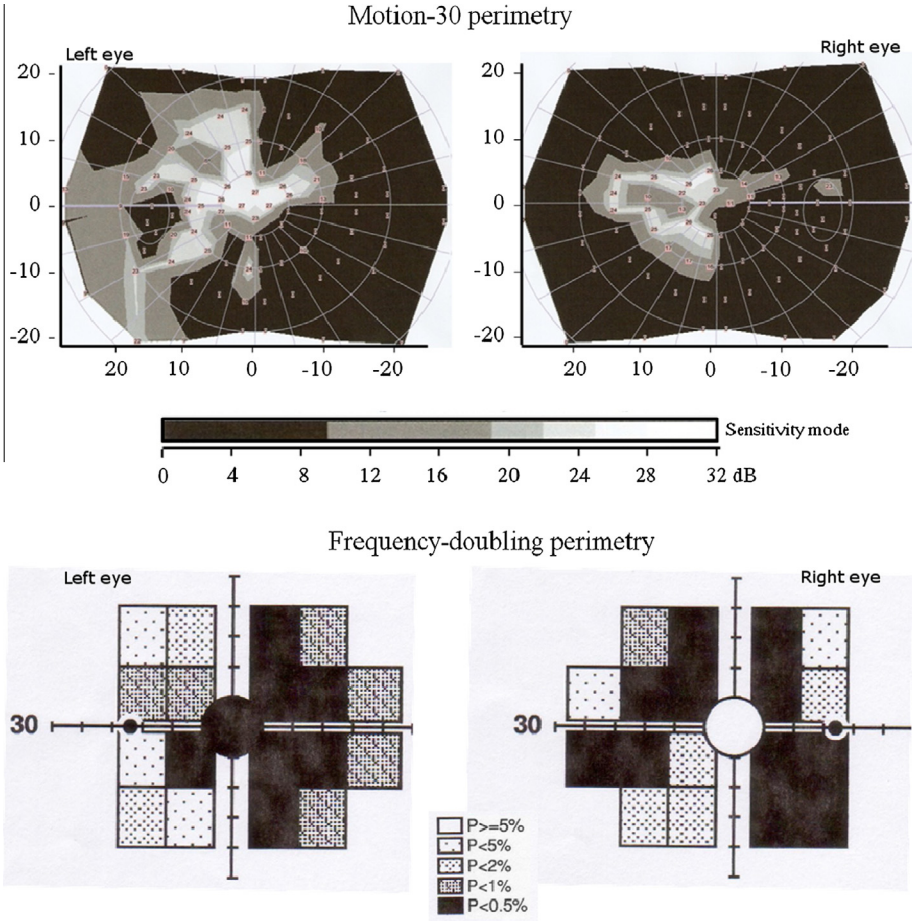

Fig. 3. Visual field motion perimetries. Upper: Motion-30 stimulus perimetry. Bottom: Frequency Doubling (FDT) perimetry (magnocellular pathway). A larger functional field deficit, including the whole right hemifield and spreading to the left hemifield (possibly following the contralateral spread of spiking activity) was observed with a motion stimulus as well as with contrast sensitivity measures of the magnocellular pathway.

of the entire contralateral visual hemifield (Dechent & Frahm, 2003; Pitzalis et al., 2006; Tootell et al., 1997; Vaina et al., 2003) unlike other retinotopic regions beyond striate cortex (V2-V3), which are quadrant-based. The anatomical localization was further corroborated by the observation of magnocellular loss in an entire visual hemifield and contralateral spread due to spiking activity. Accordingly, psychophysical testing with magnocellular/motion stimuli showed specific hemifield loss that contrasted with the peripherally confined and less extended quadrantic-like loss observed using static and color perimetry which activates the parvocellular pathway (see also Castelo-Branco et al., 2006). Parvo damage is more localized because retinotopic regions affected have dominant magno input, in particular V6, and more parvo dominated regions were relatively spared. The origin of the smaller parvo scotoma accordingly comes from another retinotopic region (V3) where both magno and parvo inputs are more balanced.

This work extends our previous evidence showing that V6 and MT belong to distinct dorsal stream pathways (Castelo-Branco et al., 2006), since in that study we found normal responses of human MT+ to motion contrast in a patient with a similar lesion location, consistent with the proposal of two distinct magnocellular dorsal stream pathways: a latero-dorsal pathway passing to MT+ and concerned with the processing of coherent motion, and a medio-dorsal pathway that routes information from V3A to the human homolog of V6 (Castelo-Branco et al., 2006). In our patient the MT/V5 region was also spared.

In sum, the functional pattern revealed by magnocellular-isolating perimetries was concordant with the evidence of damage of areas with strong magno input and hemifield representation such as V3A or V6 (Pitzalis et al., 2006; Tootell et al., 1997).

These results corroborate the notion that the cortical organization into two distinct magnocellular and parvocellular pathways goes well beyond the primary visual cortex, as suggested by animal studies (Felleman, Burkhalter, & Van Essen, 1997; Livingstone & Hubel, 1988).

The psychophysical testing of early visual pathways showed indeed that the defects dominated when motion stimuli were used. The specificity of the observed visual dissociations was consistent with similar adult-onset patterns found in the context of focal stroke (Castelo-Branco et al., 2006). We do now show that this dissociation holds for early developmental lesions with abnormal activity patterns.

Importantly, perimetric testing of dorsal stream function by using motion stimuli revealed a spreading of dysfunction to the contralateral hemifield that might be related with the BOLD inhibition in retinotopically matched regions of the contralateral hemisphere observed in EEG/fMRI data (see below).

4.2. Influence of developmental lesions on retinotopic organization

The present study also provides insights into the functional effects of epileptic discharges during brain development. In this patient, topology of retinotopic representations of V1 and V2 in affected cortex were disrupted. The relatively disorganized retinotopic pattern suggests that the early onset of abnormal electrical activity, during the development and maturation of the retinotopic

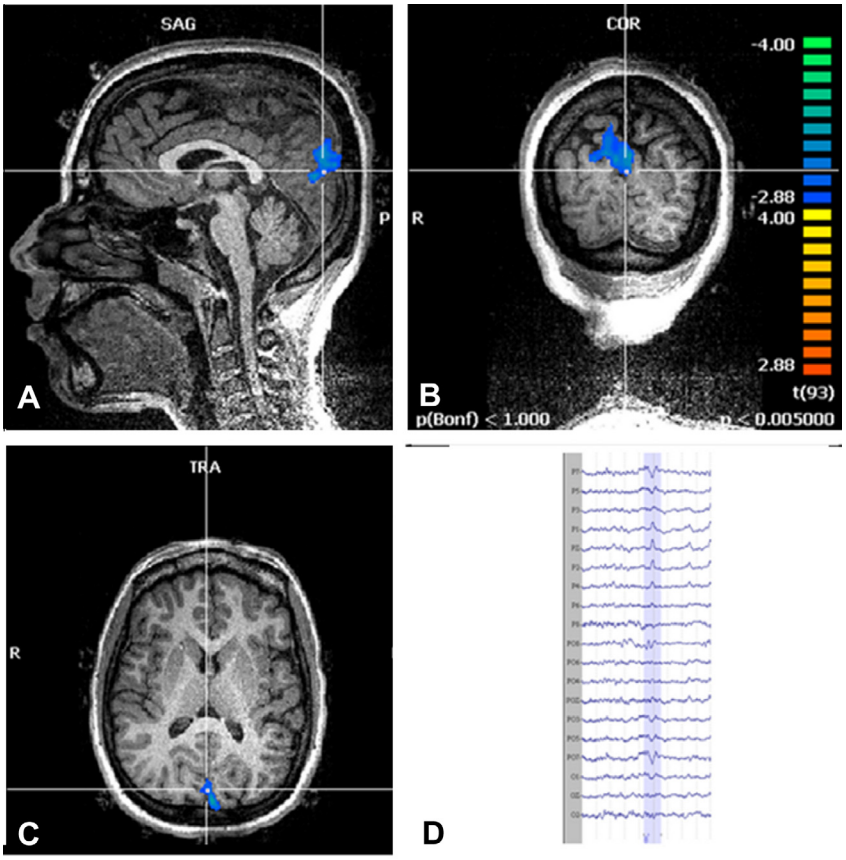

Fig. 4. Analysis of simultaneously acquired EEG and fMRI data. (A–C) Statistical maps of BOLD analysis, exhibiting deactivations in the surrounding and contralateral cortex related to interictal activity. (D) Part of EEG signal showing one epileptic spike. The fMRI model was created based on spikes identified in the EEG data.

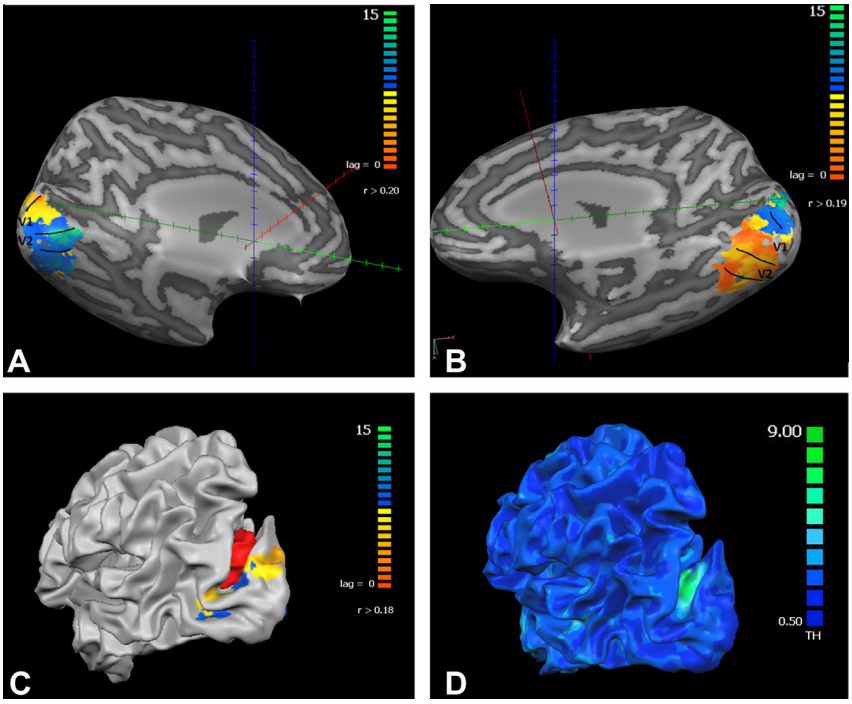

Fig. 5. Retinotopic mapping with polar angle stimuli. (A and B) Left and right hemisphere. The retinotopy showed decreased/absent activation in the dysplastic region and altered organization of neighboring left dorsal retinotopic maps. Putative V1 and V2 boundaries are delineated. (C) 3D Cortical model showing the dysplasia outlined by the neuroradiologist and the retinotopic data: no activity is present in the dysplastic cortical region (painted in red). (D) Cortical thickness analysis clearly demonstrating a region of increased cortical thickness, corresponding to the dysplasia in C.

areas, led to abnormal functional organization of neighboring visual cortex. These relative disorganization can be justified by chronic spiking-related activity, which ipsi and contralateral propagation can justify the impairments in patient's performance in the visual field psychophysical tests.

To our knowledge this is one of the first developmental retinotopic case studies (and the first in early occipital epilepsy due to cortical dysplasia), which provided the opportunity to address for the first time structure–function correlations and damage to retinotopic representations in relation to the presence of a hyperexcitable lesion. Abnormal retinotopic organization has also been documented in a study of epilepsy caused by polymicrogyria (Dumoulin, Jirsch, & Bernasconi, 2007), however no impairments in visual function could be documented to establish structure–function correlations.

Our paper agrees with the view of Tinelli et al. (2012) that congenital lesions can trigger massive reorganization of the visual system. However there is an important distinction, which is that the insult in our case is chronic due to abnormal electrophysiological activity that triggers a distinct BOLD pattern and a different form of reorganization. This may probably explain the strong difference in retinotopic organization across hemispheres (loss of topology near the lesion).

Disruption of local topology (possibly due to spiking activity) and remapping around the lesion zone (with preserved visual responses around this lesion) is remarkable. In other words, the presence of chronic spiking activity in a developing brain did not block reorganization of activity around a lesion of early onset with symptoms. Since this occurred in the first years of age this allowed for significant remapping and reorganization (as confirmed by changes in boundaries).

4.3. Negative BOLD activations: implication for the observed pattern of deficits

In fMRI, positive BOLD response has been generally associated with an increase in neuronal activity. However, several studies report negative BOLD also as a stimulus related response (Shmuel et al., 2002; Smith, Williams, & Singh, 2004) and these dominant negative effects have been reported even in cases of epilepsy when triggered by interictal spikes (Gotman, Kobayashi, Bagshaw, Bénar, & Dubeau, 2006; Marques et al., 2009; Salek-Haddadi et al., 2006). The mechanisms underlying this phenomenon are poorly understood.

The effect might be explained by a low energy requirement in the GABAergic-mediated inhibition or by a reduced synaptic activity caused by reduced neuronal input or by functional deafferentation (Gotman et al., 2006; Stefanovic, Warnking, & Pike, 2004; Logothetis, 2003).

In the present study, the spike triggered fMRI signal analysis uncovered perilesional BOLD deactivation and an unexpected and noteworthy spread of this negative BOLD to the contralateral visual cortex, to the location where contralateral magno V3A/V6 regions are located. This pattern was consistent with the contralateral spread of dorsal stream dysfunction to precisely the same regions dominated by strong magnocellular input.

Although it remains unclear why dominant negative BOLD effects are observed in several cases of epilepsy, this study suggests that EEG/fMRI does indeed provide topologically meaningful structure function correlations. Interictal activity not only induced BOLD deactivations in the surrounding cortex to the lesion but also in the retinotopically matched contralateral regions. This led to disrupted retinotopic representations in the left visual field and impaired performance. These findings are consistent with a functional interpretation of negative BOLD signals.

To our knowledge no study has described so far a relation between negative BOLD and visual functional defects.

5. Conclusions

Using multimodal methods we could identify a striking visual dissociation between early visual pathways in high level motion sensitive dorsal visual representations (up to V3A/V6). The developmental pattern of damage affected dorsal visual motion processing and occurred with a relative preservation of chromatic function. Abnormal BOLD activity patterns had a contralateral negative impact on precisely the same retinotopic magno recipient representations due to spread of abnormal activity.

This case is to our knowledge the first retinotopic study to elucidate visual reorganization and structure–function relations based on the effects of epilepsy caused by a developmental cortical dysplasia. Furthermore, it sheds light on functional segregation patterns along the visual dorsal stream and on the functional implications of negative BOLD activity. We conclude that fMRI based visual field cortical mapping allowed to find a retinotopic dissociation between chromatic and motion processing in high level dorsal visual representations, and that specific developmental damage of low and high level motion representations may occur with relative preservation of color based ventral stream function.

Acknowledgments

We would like to acknowledge the support of BIN (the Brain Imaging Network of Portugal). This work was supported by Grants CENTRO-07-ST24-FEDER-00205, PEst-C/SAU/UI3282/2013, PTDC/SAU/NEU/68483/2006 and PIC/IC/82986/2007.

References

Blanke, O., Landis, T., Mermoud, C., Spinelli, L., & Safran, A. B. (2003). Direction-selective motion blindness after unilateral posterior brain damage. *Eur. J. Neurosci., 18*(3), 709–722.

Braddick, O. J., O'Brien, J. M., Wattam-Bell, J., Atkinson, J., & Turner, R. (2000). Form and motion coherence activate independent, but not dorsal/ventral segregated, networks in the human brain. *Curr. Biol., 10*(12), 731–734.

Castelo-Branco, M., Mendes, M., Silva, M. F., Januário, C., Machado, E., Pinto, A., et al. (2006). Specific retinotopically based magnocellular impairment in a patient with medial visual dorsal stream damage. *Neuropsychologia, 44*(2), 238–253.

Dechent, P., & Frahm, J. (2003). Characterization of the human visual V6 complex by functional magnetic resonance imaging. *Eur. J. Neurosci., 17*(10), 2201–2211.

Delorme, A., & Makeig, S. (2004). EEGLAB: an open source toolbox for analysis of single-trial EEG dynamics including independent component analysis. *J. Neurosci. Methods, 134*(1), 9–21.

Diehl, B., Tkach, J., Piao, Z., Ruggieri, P., LaPresto, E., Liu, P., et al. (2010). Diffusion tensor imaging in patients with focal epilepsy due to cortical dysplasia in the temporo-occipital region: electro-clinico-pathological correlations. *Epilepsy Res., 90*(3), 178–187.

Dumoulin, S. O., Jirsch, J. D., & Bernasconi, A. (2007). Functional organization of human visual cortex in occipital polymicrogyria. *Hum. Brain Mapp., 28*(12), 1302–1312.

Felleman, D. J., Burkhalter, A., & Van Essen, D. C. (1997). Cortical connections of areas V3 and VP of macaque monkey extrastriate visual cortex. *J. Compos. Neurol., 379*(1), 21–47.

Galletti, C., Gamberini, M., Kutz, D. F., Fattori, P., Luppino, G., & Matelli, M. (2001). The cortical connections of area V6: an occipito-parietal network processing visual information. *Eur. J. Neurosci., 13*(8), 1572–1588.

Goodale, M. A., & Milner, A. D. (1992). Separate visual pathways for perception and action. *Trends Neurosci., 15*(1), 20–25.

Gotman, J., Kobayashi, E., Bagshaw, A. P., Bénar, C. G., & Dubeau, F. (2006). Combining EEG and fMRI: a multimodal tool for epilepsy research. *J. Magn. Reson. Imaging, 23*(6), 906–920.

Jones, S. E., Buchbinder, B. R., & Aharon, I. (2000). Three-dimensional mapping of cortical thickness using Laplace's Equation. *Hum. Brain Mapp., 11*(1), 12–32.

de Jong, B. M., van der Graaf, F. H., & Paans, A. M. (2001). Brain activation related to the representations of external space and body scheme in visuomotor control. *NeuroImage, 14*(5), 1128–1135.

Livingstone, M., & Hubel, D. (1988). Segregation of form, color, movement, and depth: anatomy, physiology, and perception. *Science, 240*(4853), 740–749.

Logothetis, N. K. (2003). The underpinnings of the BOLD functional magnetic resonance imaging signal. *J. Neurosci., 23*(10), 3963–3971.

Marques, J. P., Rebola, J., Figueiredo, P., Pinto, A., Sales, F., & Castelo-Branco, M. (2009). ICA decomposition of EEG signal for fMRI processing in epilepsy. *Hum. Brain Mapp., 30*(9), 2986–2996.

Newsome, W. T., & Paré, E. B. (1988). A Selective Impairment of Motion Perception Following Lesions of the Middle Temporal Visual Area (MT). *J. Neurosci., 8*, 2201–2211.

Orban, G. A., Van Essen, D. C., & Vanduffel, W. (2004). Comparative mapping of higher visual areas in monkeys and humans. *Trends Cogn. Sci., 8*(7), 315–324.

Pitzalis, S., Galletti, C., Huang, R. S., Patria, F., Committeri, G., Galati, G., et al. (2006). Wide-field retinotopy defines human cortical visual area v6. *J. Neurosci., 26*(30), 7962–7973.

Salek-Haddadi, A., Diehl, B., Hamandi, K., Merschhemke, M., Liston, A., Friston, K., et al. (2006). Hemodynamic correlates of epileptiform discharges: an EEG-fMRI study of 63 patients with focal epilepsy. *Brain Res., 1088*(1), 148–166.

Sereno, M. I., Dale, A. M., Reppas, J. B., Kwong, K. K., Belliveau, J. W., Brady, T. J., et al. (1995). Borders of multiple visual areas in humans revealed by functional magnetic resonance imaging. *Science, 268*(5212), 889–893.

Shmuel, A., Yacoub, E., Pfeuffer, J., Van de Moortele, P. F., Adriany, G., Hu, X., et al. (2002). Sustained negative BOLD, blood flow and oxygen consumption response and its coupling to the positive response in the human brain. *Neuron, 36*(6), 1195–1210.

Silva, M. F., Maia-Lopes, S., Mateus, C., Guerreiro, M., Sampaio, J., Faria, P., et al. (2008). Retinal and cortical patterns of spatial anisotropy in contrast sensitivity tasks. *Vision. Res., 48*(1), 127–135.

Simon, O. et al. (2002). Topographical layout of hand, eye, calculation, and language-related areas in the human parietal lobe. *Neuron, 33*(3), 475–487.

Smith, A. T., Williams, A. L., & Singh, K. D. (2004). Negative BOLD in the visual cortex: evidence against blood stealing. *Hum. Brain Mapp., 21*(4), 213–220.

Stefanovic, B., Warnking, J. M., & Pike, G. B. (2004). Hemodynamic and metabolic responses to neuronal inhibition. *Neuroimage, 22*(2), 771–778.

Thiele, A., Dobkins, K. R., & Albright, T. D. (2001). Neural correlates of chromatic motion perception. *Neuron, 32*, 351–358.

Tinelli, F., Cicchini, G. M., Arrighi, R., Tosetti, M., Cioni, G., & Morrone, M. C. (2012). Blindsight in children with congenital and acquired cerebral lesions. *Cortex*, 1–12.

Tootell, R. B., Mendola, J. D., Hadjikhani, N. K., Ledden, P. J., Liu, A. K., Reppas, J. B., et al. (1997). Functional analysis of V3A and related areas in human visual cortex. *J. Neurosci., 17*(18), 7060–7078.

Ungerleider, L. G., & Haxby, J. V. (1994). 'What' and 'where' in the human brain. *Curr. Opin. Neurobiol., 4*, 157–165.

Vaina, L. M., Gryzwacz, N. M., Saiviroonporn, P., LeMay, M., Bienfang, D. C., & Cowey, A. (2003). Can spatial and temporal motion integration compensate for deficits in local motion mechanisms? *Neuropsychologia, 41*(13), 1817–1836.

Vanduffel, W., Fize, D., Mandeville, J. B., Nelissen, K., Van Hecke, P., Rosen, B. R., et al. (2001). Visual motion processing investigated using contrast agent-enhanced fMRI in awake behaving monkeys. *Neuron, 32*, 565–577.

Wandell, B. A., Dumoulin, S. O., & Brewer, A. (2007). Visual field maps in human cortex. *Neuron, 56*(2), 366–383.

Wandell, B. A., & Winawer, J. (2011). Imaging retinotopic maps in the human brain. *Vision. Res., 51*(7), 718–737.

Wattam-Bell, J., Birtles, D., Nyström, P., von Hofsten, C., Rosander, K., Anker, S., et al. (2010). Reorganization of global form and motion processing during human visual development. *Curr. Biol., 20*(5), 411–415.